SSRP 2019

21. Steirisches Seminar über Regelungstechnik und Prozessautomatisierung

21st Styrian Workshop on Automatic Control

Book of Abstracts

M. Reichhartinger and M. Horn (Eds.)

September 9 - 11, 2019

Schloss Retzhof, Leitring/Wagna, Austria

ISBN: 978-3-901439-13-1

http://www.irt.tugraz.at

Graz University of Technology

Contents

Part I.

Tuesday

Implementation of Model-based Control Concepts in Continuous Pharmaceutical Engineering

Jakob Rehrl[a] **Selma Celikovic**[b] **Martin Kirchengast**[b] **Stephan Sacher**[a] **Julia Kruisz**[a] **Johannes Khinast**[a,c] **Martin Horn**[b]

Manufacturing of pharmaceutical drug products has been typically conducted in batch manner in the past. This approach shows some drawbacks like the need to store and transport intermediate material between individual batch processing steps (such as blending, granulation, etc.), a larger footprint of the production facilities and the conduction of end product testing instead of continuously monitoring the production process. Some of these drawbacks can be overcome by means of continuous manufacturing approaches, which are currently in the stage of implementation in pharmaceutical industry. These concepts allow for inline monitoring of critical process parameters (CPPs) and critical quality attributes (CQAs). Consequently, the implementation of process control concepts in order to keep the CQAs within their specification limits is enabled.

This talk presents the development of a control strategy for a hot melt extrusion (HME) and strand pelletization system, which is part of a continuous pharmaceutical production line. The overall production line is capable of producing pellets containing the active pharmaceutical ingredient (API), which are then blended with excipients and finally pressed to form tablets. The properties of the final tablets strongly depend on the size of the pellets, which is therefore considered as a CQA. Pellet size is directly influenced by the HME and pelletization step, see figure 1. By varying the intake speed of the pelletizer, the size can be adjusted. Furthermore, the strand temperature impacts the cutting quality and is therefore considered as a CPP. Appropriate strand temperature is essential for obtaining pellets that are suitable for downstream processing. A cooling track between extruder outlet and pelletizer inlet is used to keep the strand temperature close to the reference value by adjusting the cooling air mass flow.

The design and implementation of a control strategy for strand temperature and strand thickness control is presented. Pelletizer intake speed and the pressure of the cooling air are the actuators, the die temperature at the extruder outlet is considered a measurable disturbance. The system shown in figure 1 is modeled by means of the local linear model tree (LOLIMOT) algorithm [1] and a model predictive controller is designed. The size of the produced pellets is analyzed and the results obtained using the proposed control strategy are compared to the results when running the process at constant pelletizer intake speed and constant cooling air pressure.

---

[a]Research Center Pharmaceutical Engineering, Inffeldgasse 13/II, 8010 Graz, Austria, E-Mail: `jakob.rehrl@rcpe.at`, `stephan.sacher@rcpe.at`

[b]Institute of Automation and Control, Graz University of Technology, Inffeldgasse 21b/II, 8010 Graz, Austria, E-mail: `selma.celikovic@tugraz.at`, `martin.kirchengast@tugraz.at`, `martin.horn@tugraz.at`

[c]Institute of Process and Particle Engineering, Graz University of Technology, Inffeldgasse 13/III, 8010 Graz, Austria, E-mail: `khinast@tugraz.at`

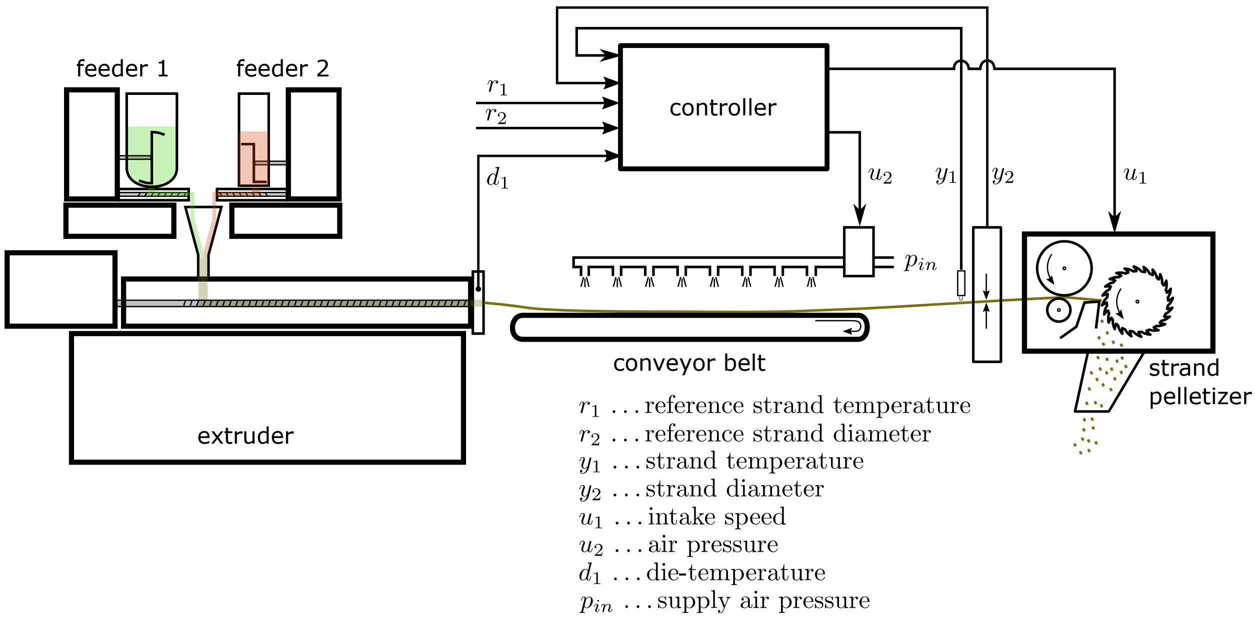

Figure 1: Sketch of the investigated process

[1] Oliver Nelles. *Nonlinear System Identification*. Springer, Berlin, Heidelberg, 2001.

Data-driven modelling of Polymer Electrolyte Membrane Fuel cells for Fault Detection

Daniel Ritzberger[a] **Stefan Jakubek**[a]

In order to extend the lifetime of polymer electrolyte membrane fuel cells (PEMFCs), especially with regard to an automotive application, advanced diagnostic methods for monitoring the operating condition are required. Electrochemical diagnostic methods [1], such as the electrochemical impedance spectroscopy (EIS), have been shown to be particularly useful and a large number of system faults can be successfully diagnosed. The electrochemical impedance describes the linear relation between current and voltage around an operating point, and is typically experimentally determined in the frequency domain by repeated single sinusoidal excitations. The experimentally determined electrochemical impedance is subsequently fitted to equivalent circuit models, as to regain an interpretability and to condense the obtained experimental data into tangible parameters for fault detection.
However, the measurement of the electrochemical impedance spectrum via EIS typically requires a significant amount of experimental time, due to the single sinusoidal excitation, during which the fuel cell system has to be operated under steady state conditions. A straightforward implementation under transient operating condition, typically encountered in an automotive application, is therefore not possible.
Alternatively, the electrochemical impedance can also be described in the discrete time domain as a difference equation, which is linear in its unknown parameters. Therefore, computationally efficient recursive estimation algorithms, such as recursive least squares (RLS), in combination with persistently exciting input signals, could be used to track the impedance during transient operations. However, it has been observed that even in the presence of moderate noise conditions the obtained impedance becomes heavily biased [2].
The reason for this is, that the noise assumption that leads to the convenient least squares estimation, is inherently incorrect for dynamic, autoregressive systems, as it is assumed that only the independent variable (output vector) is affected by noise whereas the dependent variables (regressor) are noise-free. But since for discrete time domain models past (noisy) outputs are also inputs to the system, the least squares assumption is always violated and biased parameter estimates are the result. To obtain un-biased parameter estimates in the presence of noisy model inputs, the total least squares (TLS) algorithm has been proposed [3]. As an extension to TLS, the generalized total least squares (GTLS) addresses the problem when only some regressor columns are affected by noise, whereas some are noise-free [4]. This is a useful assumption in many practical cases, for example when the additive measurement noise of input and output is differing in several orders of magnitude such that a de-correlation can become ill-conditioned, or when an intercept model with a static offset is considered. To achieve an on-line tracking of the electrochemical impedance during transient operations of the fuel cell, a recursive version of the GTLS algorithm has been developed and validated on experimental measurement of a 5cm^2 fuel cell, subjected to a generic broad-band

[a]Institute of Mechanics and Mechatronics, Workgroup of Control and Process Automation, Technische Universität Wien, Getreidemarkt 9, 1060 Vienna, E-Mail: daniel.ritzberger@tuwien.ac.at, stefan.jakubek@tuwien.ac.at

amplitude modulated pseudo random binary sequence (APRBS) excitation. It is shown, that the estimation bias due to the incorrect noise assumptions is significantly reduced [5].
To be consistent with the EIS methodology, it is further desired to transform the obtained electrochemical impedance, given as an estimated discrete time model, into an equivalent circuit model. To avoid the a-priori selection of the circuit structure and subsequent off-line fitting of parameters, an automated circuit synthesis is carried out based on the Foster synthesis [6].
With the proposed method of discrete-time model identification via GTLS and automatic synthesis of equivalent circuit models, an on-line estimation of the electrochemical impedance during transient operations can be achieved and further utilized for fault detection.

References

[1] Jinfeng Wu, Xiao Zi Yuan, Haijiang Wang, Mauricio Blanco, Jonathan J Martin, and Jiujun Zhang. Diagnostic tools in pem fuel cell research: Part i electrochemical techniques. *International journal of hydrogen energy*, 33(6):1735–1746, 2008.

[2] Björn Fridholm, Torsten Wik, and Magnus Nilsson. Robust recursive impedance estimation for automotive lithium-ion batteries. *Journal of Power Sources*, 304:33–41, 2016.

[3] Sabine Van Huffel and Philippe Lemmerling. *Total least squares and errors-in-variables modeling: analysis, algorithms and applications*. Springer Science & Business Media, 2013.

[4] Stefan Jakubek and Christoph Hametner. Identification of neurofuzzy models using gtls parameter estimation. *IEEE Transactions on Systems, Man, and Cybernetics, Part B (Cybernetics)*, 39(5):1121–1133, 2009.

[5] D Ritzberger, M Striednig, C Simon, C Hametner, and S Jakubek. Online estimation of the electrochemical impedance of polymer electrolyte membrane fuel cells using broadband current excitation. *Journal of Power Sources*, 405:150–161, 2018.

[6] Roxana Ionutiu and Joost Rommes. On synthesis of reduced order models. In *Model reduction for circuit simulation*, pages 207–223. Springer, 2011.

Adaptive Resonance-Suppression for Automotive Test Bed Systems

Klemens Kranawetter[a,b] **Richard Seeber**[a,b] **Robert Bauer**[b] **Martin Horn**[a]

The components of automotive drive lines interact through torque and angular speed. Consequently, these two quantities are at the root of many prominent concepts in automotive testing. On combustion engine test beds, for example, shaft torque and crank shaft speed frequently have to track specific reference trajectories, which may be part of a commissioning cycle or another normed testing procedure. Also among more complex testing systems, such as full vehicle or R2R ("road-to-rig") test beds, speed and torque control is crucial.

Controlling angular speed or torque in a test bed's drive line often turns out to be a demanding problem, though. At its core, the situation is one of the classics in control engineering: To achieve fast dynamics in the presence of disturbances, high-gain parameter settings are needed. High-gains, however, decrease the phase and magnitude margin, which may lead to poor performance and even stability problems. A typical scenario in this regard is shown in Fig. 1: The shaft torque in the left rear axle of an R2R test bed, which is shown in the plant-block, is controlled by a controller $\mathcal{C}$. The output of the latter is a desired profile for the electrical airgap torque, which is translated into action by an actuator in the form of an induction machine. Performance problems resulting from high controller gains can be seen in the form of shaft torque oscillations, which in the considered case occur immediately after the test bed is started.

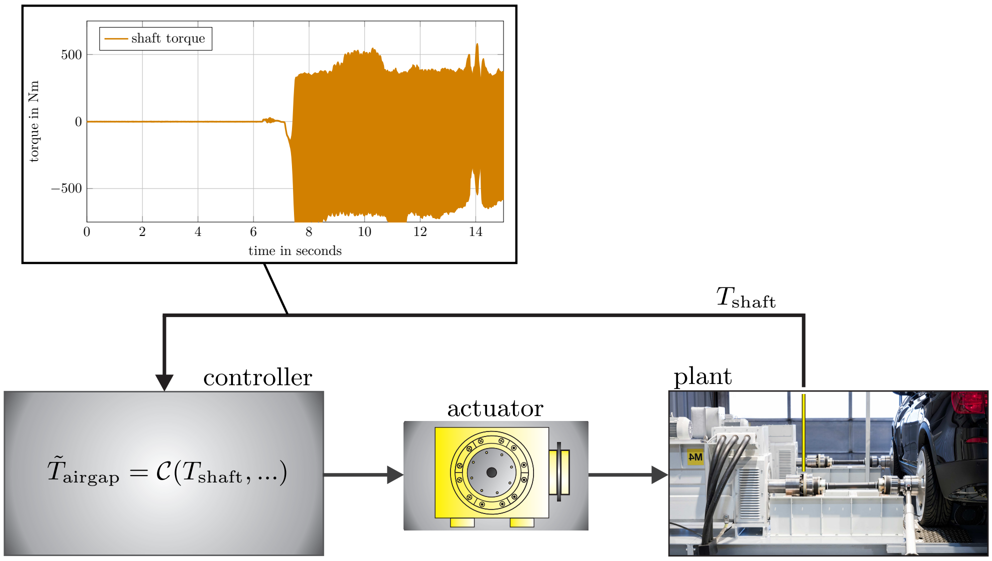

Figure 1: Torque oscillation in an R2R test bed drive line.

[a]Christian Doppler Laboratory for Model Based Control of Complex Test Bed Systems, Graz University of Technology, Inffeldgasse 21/B/I, 8010 Graz, E-Mail: `klemens.kranawetter@tugraz.at`
The financial support by the Christian Doppler Research Association, the Austrian Federal Ministry for Digital and Economic Affairs and the National Foundation for Research, Technology and Development is gratefully acknowledged.
[b]KS Engineers, Baiernstrasse 122a, 8052 Graz, E-Mail: `robert.bauer@ksengineers.at`

The frequencies that exhibit the smallest phase and magnitude margins are usually close to the resonance frequencies of the plant. Therefore, an often seen remedy against such undesired oscillations is to compensate for the resonances by the means of notch filters. This measure, however, leads to a series of follow-up questions: *Firstly*, the parameters of the used filters must be found. Due to tight commissioning schedules and the possible alteration of the plant, this step alone poses a significant obstacle. For this reason, many authors propose the use of adaptive notch filters [1, 2, 3]. *Secondly*, if an adaptive notch filter is used, it must be made sure that the filter is not influenced by external disturbances; and *thirdly*, the practical implementation must adhere to real-time constraints.

In this talk, a novel adaptive notch filtering scheme is presented, which addresses the above mentioned points. It employs a real-time capable implementation of a Blackman-windowed DFT-interpolation, and proposes a strategy to decide whether an oscillation stems from resonance or external excitation on the basis of priorly observed magnitudes. A series of experiments, which have been conducted on the test bed presented in Fig. 1, prove the algorithm's capability to identify previously unknown resonance frequencies and to suppress them appropriately. One of the obtained results is shown in Fig. 2. Therein, both dominating resonance frequencies of the associated drive line cause a growing oscillation, which is mitigated successfully in the course of the trial in each case.

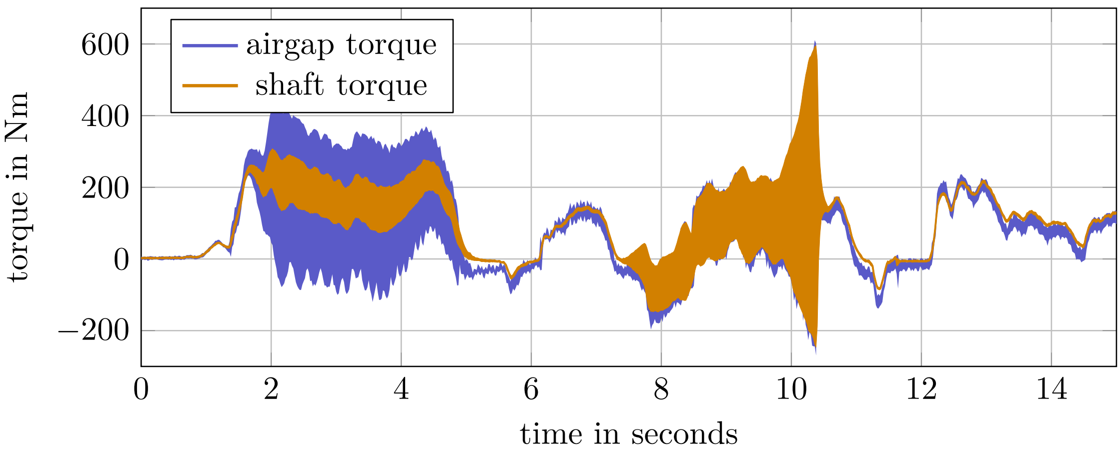

Figure 2: Measured shaft and airgap torque.

[1] Wook Bahn, Jong-Min Yoon, Nyeon-Kun Hahm, Sang-Sub Lee, Sang-Hoon Lee, and Dong-Il Cho. Application of adaptive notch filter for resonance suppression in industrial servo systems. In *2014 14th International Conference on Control, Automation and Systems (ICCAS 2014)*, pages 976–979. IEEE, 2014.

[2] Jian Kang, Songlin Chen, and Xiaoguang Di. Online detection and suppression of mechanical resonance for servo system. In *2012 Third International Conference on Intelligent Control and Information Processing*, pages 16–21. IEEE, 2012.

[3] Phillip A Regalia. A complex adaptive notch filter. *IEEE Signal Processing Letters*, 17(11):937–940, 2010.

Mechatronics and Control for Precision In-Line Metrology

Georg Schitter[a]

Scanning measurement systems, used in scientific applications as well as in the high-tech industry, demand a continuous improvement of system bandwidth and speed, range, and precision. These challenging goals can be achieved only by a proper system integration, which requires an advanced mechatronic system design and state of the art motion control. Example applications for the discussed mechatronic imaging systems are robot-based measurements with atomic force microscopy (AFM) as well as scanning laser metrology.

To meet the demanding specifications, the resulting mechatronic measurement system, including all hard- and software components, has to be tailored to and optimized for each specific application. In a scanning imaging system, for example, one can consider the various ways of performing the scanning motion in the design of the mechanical structure and selection of the actuation principle. Whether system resonances have to be avoided, damped sufficiently, or even can be utilized for the scanning motion strongly depends on the mode of operation. At the same time this influences the choice of the corresponding control system for the motion control. A proper system integration that utilizes the interplay between process design and control design is key for achieving maximum performance of mechatronic systems in the high-tech industry.

This presentation addresses these challenges by illustrating examples for scanning measurement systems utilized in in-line metrology. Taking advantage of an appropriate system integration, the presented examples successfully demonstrate the potential to enhance the performance of mechatronic imaging systems substantially by an integrated mechatronic design approach.

[a]Advanced Mechatronic Systems, Automation and Control Institute (ACIN), TU Wien, Austria, E-mail: `schitter@acin.tuwien.ac.at`

Systematic and Efficient Decision Making with Optimization

Stefan Richter[a]

Automatic decision making is ubiquitous. Applications span a wide range of industries and motivate the need for systematic tools and approaches to develop such systems. Mathematical optimization is at the core of all systematic decision making systems, be it data-based as in machine learning or model-based as in classic control.

The main benefit of an optimization-based approach is that it allows one to split the solution-seeking process into two parts: a specification part accomplished by an engineer who describes the solution characteristics and a solution-generating part that is automatically carried out by an algorithm. This split gives rise to a series of desired features such as transparent tuning, adaptability, maintainability and simplified knowledge transfer. Prevalent approaches based on heuristics and worst case assessments often cannot deliver these features.

'Efficiency' is another benefit of using optimization as, by definition, any reasonable algorithm will return an at least locally optimal decision. From experience, efficiency is secondary to systematicity in practice, but lately gains more and more of interest. Tighter regulations make over-fitting and/or wasting energy less and less an option anymore, which implies that the system has to take decisions 'at the limits' in a controlled and safe way. Again, optimization is the key enabler for such systems.

Optimization is not only applicable offline for obtaining optimal design decisions or trajectories but lately has become applicable also at runtime. Progress in hardware technology, but more than that in mathematical algorithms, has unleashed the potential of optimization for so-called embedded decision making. In order to ensure both short execution times and numerical robustness of the algorithm, embedded optimization requires a different class of algorithms compared to general-purpose solvers and also a tailoring step that aligns characteristics of the decision making problem with the algorithm.

This talk will give several examples of optimization-based decision making from diverse industries at a high level and explain the specific challenges. In addition, a more detailed theoretic treatment of a specific fast and numerically robust algorithm for solving practical embedded linear model predictive control problems will be provided. By means of a subsea separator control problem it is exemplified that runtimes in the range of milliseconds can be achieved even on low-cost control hardware. Further details of this algorithm can be found in [1, 2].

[1] D. Kwame Minde Kufoalor, S. Richter, Lars Imsland, and Tor Arne Johansen. Structure exploitation of practical MPC formulations for speeding up first-order methods. In *56th IEEE Annual Conference on Decision and Control, CDC 2017, Melbourne, Australia, December 12-15, 2017*, pages 1912–1918, 2017.

[2] Stefan Richter. Structure Exploitation of Practical MPC Formulations for Fast and Efficient First-Order Methods. Technical report, Richter Optimization GmbH, Zurich, Switzerland, 2016. Available at `http://www.richteroptimization.com/public/techreport_structure_exploit.pdf`.

[a]Richter Optimization GmbH, Furttalstrasse 29, 8046 Zurich, Switzerland, E-mail: sr@richteroptimization.com, Website: www.richteroptimization.com

Part II.

Wednesday morning session

Robust consensus-based Secondary Frequency and Voltage Restoration of Inverter-based Islanded Microgrids

Milad Gholami, Alessandro Pilloni, Alessandro Pisano, Elio Usai

I. Extended Abstract

MICROGRIDs (MGs) are low-voltage electrical networks in which distributed generation, often by renewable micro-sources such as wind turbines, fuel cells and photovoltaic panels, supply a number of loads and storage systems.

Such networks are characterised by a high variability of the resources, and the absence of a main synchronous generator which imposes both, the frequency ω_i and the output voltage v_i of each Distributed Generator (DG), denoted by "i", and operating over the MG. Therefore, proper control laws have to be designed to guarantee the regulation of the main electrical parameters of each DG towards pre-specified reference signals

$$v_{ref} = v_i = v_k \quad \forall\ i,k \in \mathcal{V} = 1,2,\ldots,n \tag{1}$$

$$\omega_{ref} = \omega_i = \omega_k \quad \forall\ i,k \in \mathcal{V} = 1,2,\ldots,n \tag{2}$$

while satisfying the load distribution among generators [5,8].

In recent years a number of control approaches aimed to address the voltage and frequency restoration problem in MGs, also referred to as *Secondary Control* (SC) problem have been proposed. These are mainly based on simplified models of the network dynamics [1-4]. However, since the network parameters are subjected to uncertainties and distributed in space, multi-agents based cooperative robust control techniques have been considered as an effective approach to the problem [5-8]. However, the cited approaches could lose their effectiveness whenever delays occur in the communication infrastructure. To limit or compensate the effect of packet loss, and latency in communication some interesting approaches such as [9,10] have been proposed in the multi-agent systems field, and which application in the context of MGs appear promising, with some ad-hoc modifications.

In this research we first resume the results in [8], where novel control strategies to perform the exact finite-time SC problem among voltages (1), and frequencies (2), in an inverter-based islanded MG have been presented. There, the problem is faced from a cooperative-based control perspective inspired to the tracking consensus paradigm, and sliding-mode-based distributed algorithms are designed to enhance the robustness and convergence properties of the electrical system in a distributed way. The knowledge of the distributed generators' models and line parameters were dispensed with, but delayed communications among DGs were not considered.

Here, to take into account delays in the communication network that connects the distributed controllers, the robust approach in [8] is revisited and integrated by an inherently robust Integral Sliding Mode Control (ISMC) term [11],

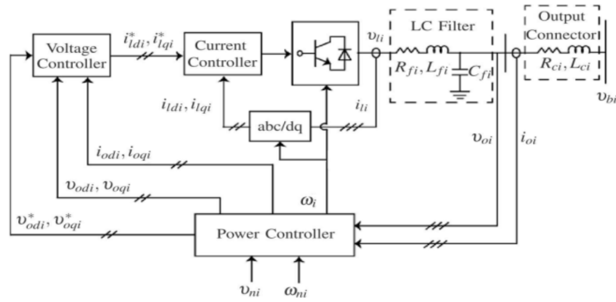

Fig. 1. DG's PC block diagram, where v_{ni} e ω_{ni} denote the voltage and frequency PC's reference signals provided by the SC layer.

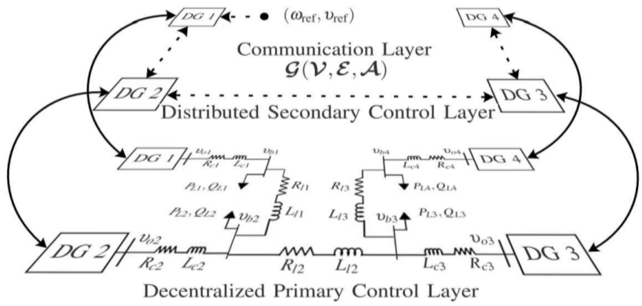

Fig. 2. A MG system of four DGs with a multi-agent based SC layer.

exploiting the performance of the Primary Control (PC) devoted to regulate the inverter-based connection of the generator with the network.

The method is fully distributed, and thanks to an artificial increase of the DG's input-output relative degree that allows for designing the control in terms of its derivative, results that the actual control output is continuous and can be safely Pulse-Width Modulated (PWM) by a fixed given frequency, as required to not hurt the switching power artifacts.

To corroborate the results a dedicated Lyapunov analysis providing a simple set of tuning rules is given. A Linear Matrix Inequality (LMI) criterion is also employed to estimate the maximum delay for communications.

II. Microgrid Modellization

II.A Distributed Generators (DGs) model. Generally, the DG's modellization for SC purposes includes: a prime dc-source, a 3-ph dc/ac power converter, a RLC filter, a RL output connector and the local PC, consisting of three nested control loops that control, as shown in Fig. 1, the DG's power flows, voltages, and currents at the connection point of the MG. The PC is designed by using only local measurements with the aim to guarantee the power grid stability while preserving the power sharing facilities [2,5]. Taking into account the bandwidth separation within current and voltage dynamics, the DG's dynamics can be approximatively represented as follows [5],

$$\begin{aligned} \dot{\delta}_i &= \omega_i = \omega_{ni} - k_{P_i} \cdot P_i^m \\ k_{v_i} \cdot \dot{v}_i &= -v_i + v_{ni} - k_{Q_i} \cdot Q_i^m \end{aligned}, \tag{3}$$

where k_{P_i} and k_{Q_i} are the PC's droop parameters designed for a proper power sharing. P_i^m and Q_i^m denote the dc components of the instantaneous active and reactive power flows P_i, Q_i, measured at the output port of the i-th DG through a low-pass filter device with time-constant τ_{P_i} and τ_{Q_i}, resp., as

$$\begin{aligned} \tau_{P_i} \cdot \dot{P}_i^m &= -P_i^m + P_i \\ \tau_{Q_i} \cdot \dot{Q}_i^m &= -Q_i^m + Q_i \end{aligned}. \tag{4}$$

II.B Networks models. Following the MG diagram depicted in Fig. 2, both the communication and the electrical network can be represented by a graph $\mathcal{G}(\mathcal{V},\mathcal{E})$ where $\mathcal{V}$ is the set of vertexes, $\mathcal{E}$ the set of edges. $\mathcal{N}_i$ denotes set of neighbours of the i-th vertex. The resulting two graphs could be different, but guaranteeing the network connectivity. The electrical network connections allows for the power transfer among the DGs bars according to

$$P_i = P_{L_i} + \textstyle\sum_{k \in N_i} v_i v_k \cdot B_{ik} \cdot \sin(\delta_i - \delta_k) \tag{5}$$

$$Q_i = Q_{L_i} + v_i^2 \cdot B_{ii} + \textstyle\sum_{i \in N_i} v_i v_k \cdot B_{ik} \cdot \cos(\delta_i - \delta_k). \tag{6}$$

where v_i and δ_i met (3), and P_{L_i}, Q_{L_i} denote the local loads at output port of the i-th DG. Finally B_{ik} is the power line susceptance assumed to be positive if inductive [1,5].

From (5) and (6) it is evident how the presence of loads and connections causes variations on the frequency and voltage dynamics in accordance with (3) and (4).

On the other hand, the communication network is such that it exist at least one node, refereed as "0", which is globally reachable in the augmented graph $\mathcal{G}'$ which vertex set is $\mathcal{V}' = \{0\} \cup \mathcal{V}$. Node "0" makes the role of the leader in the SC network, and it can send the SC reference signals just to a subset of DGs, as shown for instance in Fig. 2.

III. Proposed Secondary Control Strategy

In the absence of a SC layer all the DGs' frequencies and voltages deviate from their nominal reference values (1), (2). To perform the SC objectives (1)-(2) on an islanded MG while preserving the active power sharing among DGs [5,8]

$$m_i P_i = m_k P_k \leftrightarrow \omega_{ni} = \omega_{nk} \quad \forall\ i,k \in \mathcal{V}, \tag{7}$$

which correspond to a further constraint on the frequency control inputs ω_{ni}, two novel time-delay based distributed tracking SC protocols have been proposed. Respectively, the proposed voltage SC is

$$\begin{aligned} \dot{v}_{ni}(t) &= -\alpha_i^v \cdot sign\big(\dot{v}_i(t) + v_i(t) - z_i^v(t)\big) + u_i^v(t) \\ \ddot{z}_i^v(t) &= \dot{v}_i(t) + u_i^v(t) \\ u_i^v(t) &= -\textstyle\sum_{k \in N_i'}\big[k_{ik}^v\big(v_i(t-\tau_{ik}) - v_k(t-\tau_{ik})\big)\big] \\ &\quad -\textstyle\sum_{k \in N_i'}\big[k_{ik}^{\dot{v}}(\dot{v}_i(t-\tau_{ik}) - \dot{v}_{ik}(t-\tau_{ik}))\big] \\ \dot{k}_{ik}^v &= |v_i(t-\tau_{ik}) - v_k(t-\tau_{ik})|^2 \\ \dot{k}_{ik}^{\dot{v}} &= |\dot{v}_i(t-\tau_{ik}) - \dot{v}_k(t-\tau_{ik})|^2 \end{aligned}, \tag{8}$$

where $\alpha_i^v \in \Re^+$ is a constant gain chosen large enough to dominate the bounds of the uncertainties in the voltage dynamics (3)-(6), similarly with [8]. In (8) is evident the presence of delays in the communication among the SC of each DG. τ_{ik} is the time-varying delay in the communication between the i-th and the k-th DG, such that $|\dot{\tau}_{ik}| \leq \tau^*$. Similarly to (8), the proposed frequency SC is

$$\begin{aligned} \dot{\omega}_{ni}(t) &= -\alpha_i^\omega \cdot sign\big(\omega_i(t) - z_i^\omega(t)\big) + u_i^\omega(t) \\ \dot{z}_i^\omega(t) &= u_i^\omega(t) \\ u_i^\omega(t) &= -\textstyle\sum_{k \in N_i'}\big[k_{ik}^\omega\big(\omega_i(t-\tau_{ik}) - \omega_k(t-\tau_{ik})\big)\big] \\ &\quad -\textstyle\sum_{k \in N_i'}\big[k_{ik}^{\omega_n}(\omega_{ni}(t-\tau_{ik}) - \omega_{ni}(t-\tau_{ik}))\big] \\ \dot{k}_{ik}^\omega &= |\omega_i(t-\tau_{ik}) - \omega_k(t-\tau_{ik})|^2 \\ \dot{k}_{ik}^{\omega_n} &= |\omega_i(t-\tau_{ik}) - \omega_k(t-\tau_{ik})|^2 \end{aligned}, \tag{9}$$

where $\alpha_i^\omega \in \Re^+$ is constant gain, chosen to dominate the bounds of the uncertainties in the frequency dynamics (3), (4), and (5). By means of a dedicated Lyapunov it can be shown that if α_i^v and α_i^ω dominate the DG's local uncertainties (4)-(6), a feasible set of Linear Matrix Inequalities (LMIs) exists which confirm the attainment of the SC objectives (1), (2), (7).

IV. Conclusions

A novel robust distributed SC architecture for inverter-based islanded MGs is proposed. The method improve the current State of the Art because it is fully distributed, model-free, and robust against delayed directed communications and parameters uncertainties. Moreover, since the control actions are continuous, they can be safely Pulse-Width Modulated by a fixed given frequency as needed to not hurt the switching power artifacts.

Further investigations on this activity will focus on the design of distributed Tertiary Control (TC) layers for the optimal economic dispatch of power among DGs in the presence of communication delays and active and reactive power sharing constraints.

References

[1] J.W. Simpson-Porco , F. Dörfler, F. Bullo, "Voltage stabilization in microgrids via quadratic droop control," IEEE Trans. Autom. Control, 62(3) : 1239–1253, 2017.

[2] A. Bidram, A. Davoudi, "Hierarchical structure of microgrids control system," IEEE Trans. Power Syst., vol. 3, no. 4 : 1963–1976, 2012.

[3] J.M. Guerrero, M. Chandorkar, T.-L. Lee, P.C. Loh, "Advanced control architectures for intelligent microgrids: Decentralized and hierarchical control," IEEE Trans. Ind. Electron., 60(4) : 1254–1262, 2013.

[4] F. Dörfler, J.W. Simpson-Porco, F. Bullo, "Breaking the hierarchy: Distributed control and economic optimality in microgrids," IEEE Trans. Control Netw. Syst., 3(3) : 241–253, 2016.

[5] F. Guo, C. Wen, J. Mao, Y. Song. "Distributed secondary voltage and frequency restoration control of droop-controlled inverter-based microgrids," IEEE Trans. Ind. Electron., 62(7), : 4355–4364, 2015.

[6] H. Bevrani, M.R. Feizi, S. Ataee, "Robust Frequency Control in an Islanded Microgrid: H∞ and μ-Synthesis Approaches", IEEE Trans. Smart Grid, 7(2) : 706 - 717, 2016.

[7] M. Cucuzzella, G.P. Incremona, and A. Ferrara, "Decentralized Sliding Mode Control of islanded AC microgrids with arbitrary topology", IEEE Trans. Ind. Electronics, 64(8) : 6706–6713, 2017.

[8] A. Pilloni, A. Pisano, and E. Usai, "Robust finite-time frequency and voltage restoration of inverter-based microgrids via sliding-mode cooperative control," IEEE Trans. Ind. Electron., 65(1) : 907–917, 2018.

[9] E.A.A. Coelho, D. Wu, J.M. Guerrero, J.C. Vasquez, T. Dragičević, Č. Stefanović, and P. Popovski, "Small-signal analysis of the microgrid secondary control considering a communication time delay," IEEE Trans. Ind. Electron., 63(10) : 6257–6269, 2016.

[10] A. Petrillo, A. Salvi, S. Santini, A.S. Valente, "Adaptive synchronization of linear multi-agent systems with time-varying multiple delays," Journal of the Franklin Institute, 354(18) : 8586–8605, 2017.

[11] A. Pilloni, A. Pisano, M. Franceschelli, E. Usai, "Integral sliding modes for the robustification of consensus-based multi-agent based systems," Int. Workshop on Variable Structure Systems, 1(1) : 222–227, 2016.

Parameter Preference for the Super-Twisting Algorithm Induced by $\mathcal{H}_\infty$-Norm Analysis

Daipeng Zhang[a] **Johann Reger**[a]

Sliding mode algorithms (SMAs) can provide finite time convergence (FTC) for the sliding variable under certain type of matched disturbance. Here the super-twisting algorithm (STA), when designed as controller, ensures FTC for a Lipschitz-continuous matched disturbance while maintaining the control signal continuous [1]. The STA can also be built as an observer and offer exact estimation in finite time [2]. In our contribution we examine

$$\begin{aligned} \dot{x}_1 &= -k_1\lceil x_1\rfloor^{\frac{1}{2}} + x_2, \\ \dot{x}_2 &= -k_2\lceil x_1\rfloor^{0} + b\,\phi. \end{aligned} \tag{1}$$

Such STA enjoys the property of a linear-like structure by employing the state transformation $\xi = \left(\lceil x_1\rfloor^{\frac{1}{1-d}}, x_2\right)^\top$, see [3], and the property of homogeneity [4]. The necessary and sufficient condition for a stabilizing parameter set when subject to a matched disturbance can be found in [5], providing a lower bound that guarantees FTC under matched disturbance. However, if the disturbance does not always obey this bound, then the state will be excited. In this case, an optimal choice for the parameters is possible. Our goal is to explore this topic in order to obtain such optimal parameters based on some criteria.

Main result

Using the state transformation from [3], the authors of [6] have applied the $\mathcal{H}_\infty$-norm

$$\lambda(k_1, k_2) = \sup_{\phi\in\Phi} \frac{\|E\xi\|_2}{\|\phi\|_2} \quad \text{with} \quad E = \operatorname{diag}\left(\sqrt{E_1}, \sqrt{E_2}\right) \tag{2}$$

on the STA for a disturbance $\phi \in \mathcal{L}_2$ with $k_2 < |b\phi(t)| < M,\ t \in [t_0, t_1]$ for some finite M and $|b\phi(t)| \le b,\ t \in \mathbb{R}\backslash[t_0, t_1]$ and proposed an $\mathcal{H}_\infty$-norm optimal parameter range for the STA. The derivation involves keeping the value function

$$J_\lambda = \dot{V}_\lambda + E_1|x_1|^{\frac{2}{1-d}} + E_2|x_2|^2 - \lambda^2|\phi|^2 \le 0, \tag{3}$$

where $V_\lambda = \xi^\top P\xi$ is in quadratic form. This inequality is equivalent to solving the following algebraic Riccati equation when assuming $|x_1| \le x_b$ during evolution of state, i.e.

$$PA + A^\top P + x_b^{\frac{-d}{1-d}} E^\top E + x_b^{\frac{-d}{1-d}} \lambda^{-2} PBB^\top P = 0 \tag{4}$$

may be solved resorting to its corresponding Hamilton matrix. The problems are:

1. Though the $\mathcal{H}_\infty$-norm optimal parameters are homogeneous functions of degree 0, the optimal λ is not of homogeneous degree 0. Thus, it is a local bound and input-sensitive.

[a]Fachgebiet Regelungstechnik, Technische Universität Ilmenau, Helmholtzplatz 5, D-98693 Ilmenau, E-Mail: {daipeng.zhang,johann.reger}@tu-ilmenau.de

2. The simulation has shown that the optimal point for observer design problem is shifted due to this reason.

In order to overcome such problems, we advocate the use of an other $\mathcal{H}_\infty$-norm of the form

$$\gamma(k_1, k_2) = \sup_{\phi \in \Phi} \frac{\|E\xi\|_2}{\|\lceil \phi \rfloor^{\frac{1}{1+d}}\|_2}, \tag{5}$$

which is homogeneous of degree 0, and study the similar idea of keeping

$$J_\gamma = \dot{V}_\gamma + E_1 |x_1|^{\frac{2}{1-d}} + E_2 |x_2|^2 - \gamma^2 |\phi|^{\frac{2}{1+d}} \leq 0, \tag{6}$$

$$V_\gamma = a_1 \Big(\tfrac{1-d}{2-d} |x_1|^{\frac{2-d}{1-d}} - a_{12} x_1 x_2 + \tfrac{a_2}{2-d} |x_2|^{2-d} \Big). \tag{7}$$

Here γ is constant, thus, this way we overcome the problem of input sensitivity of former λ. We show that such γ

1. can be applied to the second order SMA in general form (SOSMA):

$$\begin{aligned} \dot{x}_1 &= -k_1 \lceil x_1 \rfloor^{\frac{1}{1-d}} + x_2, \\ \dot{x}_2 &= -k_2 \lceil x_1 \rfloor^{\frac{1+d}{1-d}} + b\,\phi. \end{aligned} \tag{8}$$

   The SOSMA captures the linear case and the STA, as extreme cases. We study γ in the SOSMA by approaching the STA in a limit sense to study the behavior of the STA.

2. can only be calculated numerically by carrying out a unit-sphere search, thus lacking the analytical result available for λ (not published).

When combining both $\mathcal{H}_\infty$-norms, we can support a conclusion on the optimal parameter choice derived for λ by calculating and comparing γ from various choices of parameter.

References

[1] X. Yu and M. Önder Efe, (Eds.). *Recent Advances in Sliding Modes: From Control to Intelligent Mechatronics*, Springer, 2015.

[2] J. Davila, L. Fridman, and A. Levant, “Second-order sliding-mode observer for mechanical systems,” *IEEE Transactions on Automatic Control*, vol. 50, no. 11, pp. 1785–1789, 2005.

[3] J.A. Moreno and M. Osorio, “A Lyapunov approach to second-order sliding mode controllers and observers,” in *Conference on Decision and Control*, 2008, pp. 2856–2861.

[4] A. Bacciotti and L. Rosier, *Lyapunov Functions and Stability in Control Theory*, Springer, 2005.

[5] R. Seeber and M. Horn, “Necessary and sufficient stability criterion for the super-twisting algorithm,” in *15th International Workshop on Variable Structure Systems (VSS)*, Graz, Austria, 2018, pp. 120–125.

[6] D. Zhang and J. Reger, “$\mathcal{H}_\infty$-Optimal Parameters for the Super-Twisting Algorithm with Intermediate Disturbance Bound Mismatch,” in *15th International Workshop on Variable Structure Systems (VSS)*, Graz, Austria, 2018, pp. 303–308.

An infinite-dimensional output feedback tracking controller for a pneumatic system with distributed parameters

Nicole Gehring[a] **Richard Kern**[b]

In industrial applications, due to constructive and fiscal restrictions, the spatial distance between pneumatic actuators and the corresponding compressed air supply is usually quite significant. This alignment complicates the control of such systems, in particular driving the pneumatic actuator. In a simplified set-up, this challenge is emulated at a test-bench at Technical University of Munich (see Fig. 1). Therein, a tank stands place of the pneumatic actuator. The compressed air is supplied by an external pressurized air reservoir. The goal is to control the valve such that a desired pressure trajectory is tracked in the tank, despite of the considerable tube length of 5 m connecting the two components. For that, only a measurement of the air pressure downstream of the valve is available.

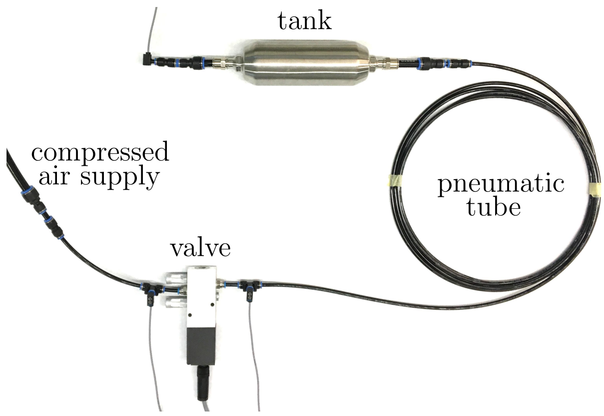

Figure 1: A photo of the main components of the test bench.

A mathematical description of the test bench is derived using the conservation of mass, momentum and energy. Based on several idealizing assumptions, finally, a linear model is obtained that comprises a second-order partial differential equation (PDE) of hyperbolic type for the tube and a first-order ordinary differential equation (ODE) for the tank (see [4]). Assuming a normalized spatial coordinate $z \in [0, 1]$, the density $\rho(z, t)$ and the momentum density $(\rho v)(z, t)$ satisfy

$$\begin{aligned}
\partial_t \rho(z,t) - \tfrac{1}{L}\partial_z(\rho v)(z,t) &= 0\\
\partial_t(\rho v)(z,t) - \tfrac{a_{\mathrm{iso}}^2}{L}\partial_z \rho(z,t) &= -k_{\mathrm{fric}}\tfrac{32\eta_0}{D^2}\tfrac{1}{\rho_0}(\rho v)(z,t)\\
\tfrac{d}{dt}\rho(0,t) &= \tfrac{A}{V_{\mathrm{vol}}}(\rho v)(0,t)\\
(\rho v)(1,t) &= \tfrac{1}{A}U(t)\\
Y(t) &= R_{\mathrm{s}} T_0 \rho(1,t).
\end{aligned}$$

[a]Institute of Automatic Control and Control Systems Technology, Johannes Kepler University Linz, Altenburger Straße 69, 4040 Linz, Austria, email: nicole.gehring@jku.at

[b]Chair of Automatic Control, Technical University of Munich, Boltzmannstr. 15, 85748 Garching/Munich, Germany, email: richard.kern@tum.de

For such systems of bidirectionally coupled ODEs and PDEs, recently, backstepping methods have been suggested, both, for the state feedback and for the state observer design, e.g. [3, 2, 1]. In [5] and [6], the approach is applied to the linear model of the pneumatic test bench. The combined state feedback and state observer results in an infinite-dimensional output feedback controller. In order achieve fast pressure (and such density) changes in the tank, this controller is augmented by a flatness-based feedforward controller (cf. [7] and [5]).

The talk delineates the entire model-based design starting with the derivation of the mathematical model, the design of the backstepping-based output feedback and the flatness-based feedforward controller, and, finally, the implementation and experimental validation of the infinite-dimensional output feedback tracking controller at the test bench.

[1] J. Deutscher, N. Gehring, and R. Kern. Output feedback control of general linear heterodirectional hyperbolic ODE-PDE-ODE systems. *Automatica*, 95:472–480, 2018.

[2] J. Deutscher, N. Gehring, and R. Kern. Output feedback control of general linear heterodirectional hyperbolic PDE-ODE systems with spatially-varying coefficients. *Int. J. Contr.*, in press, 2019.

[3] F. Di Meglio, F. Bribiesca Argomedo, L. Hu, and M. Krstic. Stabilization of coupled linear heterodirectional hyperbolic PDE-ODE systems. *Automatica*, 87:281–289, 2018.

[4] R. Kern. Physical modelling of a long pneumatic transmission line: models of successively decreasing complexity and their experimental validation. *Math. Comput. Model Dyn. Syst.*, 23:536–553, 2017.

[5] R. Kern and N. Gehring. Tracking control for a long pneumatic transmission line. In *Proc. 22nd International Conference on Methods and Models in Automation and Robotics (MMAR)*, pages 180–185, 2017.

[6] R. Kern, N. Gehring, J. Deutscher, and M. Meißner. Design and experimental validation of an output feedback controller for a pneumatic system with distributed parameters. In *Proc. 18th International Conference on Control, Automation and Systems (ICCAS), PyeongChang, Korea, October 17-20, 2018*, pages 1391–1396, 2018.

[7] T. Knüppel and F. Woittennek. Control design for quasi-linear hyperbolic systems with an application to the heavy rope. *IEEE Trans. Autom. Control*, 60:5–18, 2015.

Passive Radar for Air Surveillance

Dietrich Fränken, Oliver Zeeb

Hensoldt Sensors, Ulm, Germany

{dietrich.fraenken, oliver.zeeb}@hensoldt.net

***Abstract*—HENSOLDT has developed a passive radar system based on analog and digital audio and/or video broadcasting stations that is capable to detect and track, in real-time, airliners, small and maneuvering aircraft as well as fighters alike. This presentation recalls the underlying principles of passive radar and briefly sketches the main challenges to be dealt with. Results obtained with a cluster of four stations will demonstrate tracking capabilities and overall surveillance performance.**

I. INTRODUCTION

Passive radar (PR) systems rely on third-party transmitters such as analog or digital audio or video broadcasting stations to illuminate targets of interest, see [1], [2]. Fig. 1 shows three variants of an integrated FM/DAB/DVB-T passive radar system for airspace surveillance tasks developed by HENSOLDT. Each single sensor processes data received from up to 16 FM transmitters and 5 DAB/DVB-T single frequency networks (SFN) in real-time, see [3], [4]. Cluster operation with multiple sensor stations is also possible where several of those stations can be combined to create a common air situation picture.

Fig. 1. Passive radar setups: mobile vehicle, portable, stationary

This presentation focusses on tracking and data fusion in the system. It begins with the explanation of bistatic observations and how to obtain Cartesian 3D target position and velocity estimates from that data. The major building blocks of the tracking and data fusion software within the HENSOLDT PR system will be described giving some insight into the tasks they have to perform. Selective illustrative tracking results from live trials with a sensor cluster conclude this presentation. They are the outcome of the significant progress that has been achieved in all parts of the processing chain within the HENSOLDT passive radar system from the antenna design over analog and digital receivers as well as signal processing down to the tracking and data fusion detailed here.

II. FROM BISTATIC TO CARTESIAN DATA

A PR station measures the time-difference of arrival (TDoA) between the signal received directly from an illuminator (having unknown signal emission time) and the echo reflected from a target. For a target located at position $\mathbf{p}$ according to Fig. 2, the total covered distance r of the reflected signal from illuminator to sensor (dashed lines) can be computed from the measured TDoA Δt via $r = c \cdot \Delta t + L$ where c is the known propagation speed of the emitted electromagnetic waves and L is the known distance between illuminator and sensor. In addition to the bistatic range r, the HENSOLDT passive radar system measures Doppler and herewith the (bistatic) range-rate $\dot{r}$ plus an azimuth (by means of digital beam-forming).

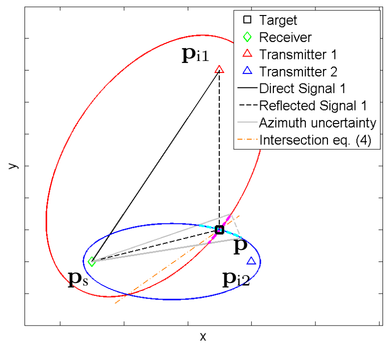

Fig. 2. Bistatic data from sensor/illuminator pairs.

In order to obtain a 3D Cartesian estimate, data from several illuminators is accumulated. Therein, each bistatic range measurement defines an ellipsoid (in 3D) with sensor and illuminator positions as focal points and the target on the ellipsoid as indicated in Fig. 2. While (three or more) ellipsoids from different sensor/illuminator pairs would lead, in theory, to one unique intersection point (the true target location), this is most unlikely to occur in practice as the measured data is prone to statistical measurement errors (for FM, the range error may be 1 km or more). To solve this issue, the HENSOLDT PR system obtains initial 3D position estimates by using two measurements in combination with a configured set of z-planes. Each of these defines a 2D intersection problem and, by also honoring the measured range-rate as well as measurement errors, yields up to four 3D Cartesian (position plus velocity) estimates including uncertainties. Those are then successively updated with further bistatic measurements. Overall, a Gaussian mixture approach is thus applied to initiate tracks for targets with unknown height (cf. [5], [6]).

III. Tracking and Data Fusion

The discussion so far only considers the one-target case. In real life, the general multi-target case for a larger number of illuminators with unknown measurement-to-target associations plus the frequent occurrence of clutter measurements quickly lead to an extremely high number of possible intersection hypotheses to be monitored and evaluated. Fig. 3 shows some typical measured bistatic data. Tracking and data fusion has to decide which combinations of reports from different illuminators to actually use for obtaining Cartesian estimates.

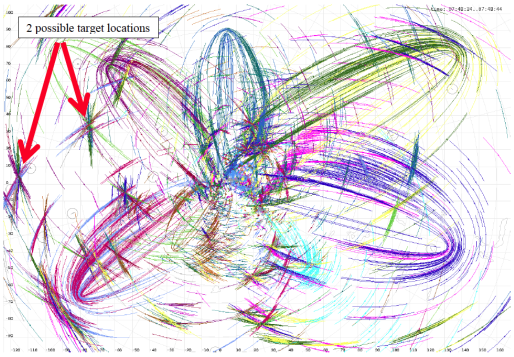

Fig. 3. Bistatic data accumulated over 10 seconds: 2D position from measured bistatic range and azimuth with an ellipse sector caused by azimuth uncertainty.

Fig. 4 displays the software architecture of the tracking and data fusion software used in the HENSOLDT passive radar system. Details regarding the different processing stages will be given in the presentation and can be found in [7]–[9] and the references therein.

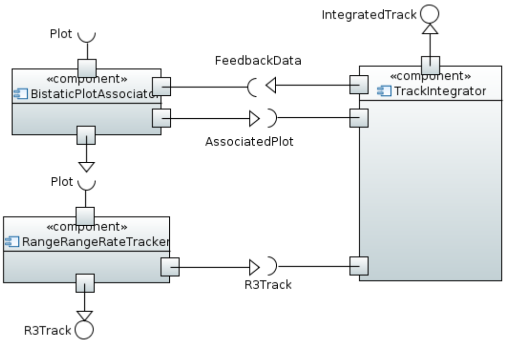

Fig. 4. Software architecture and building blocks.

In the Bistatic Plot Associator, plots entering the tracking system are matched to already existing 3D tracks. Plots associated this (globally optimal) way are sent directly to the Track Integrator and used to update the 3D tracks therein, the remaining plots (stemming from new targets or clutter) are processed in the Range/Range-Rate Tracker. In that unit, range/range-rate tracks (R^3 tracks) are formed, i. e., consistent trails are sought in the measurement data. Confirmed R^3 tracks enter the Track Integrator. This unit fulfils the major task of computing and monitoring the Gaussian mixtures (including their likelihoods) coming with all association hypotheses and finally deciding on which of those can be confirmed to build Cartesian tracks. The latter ones are fed back to the Bistatic Plot Associator and sent to the HMI for output.

IV. Some Tracking Results

Fig. 5 depicts some recent results obtained in real-time during live-trials with a cluster of four HENSOLDT passive radar stations three of which were located around Munich and one near Ulm in Southern Germany. No other data than the PR data has been used to generate the presented results. The obtained air target situation picture, accumulated over one hour, spans an area of around 500 km in diameter. The shown dogfight lasted about 10 minutes. Due to their relatively close distance, the tracks of two aircraft can hardly be separated visually during most of the time. A third fighter, displayed in orange, is present in this scene making a 4.5g turn in the upper part of the picture. The frequent track update rate of 0.5 seconds (being high in comparison to rotating active surveillance radars with typical scan times above 4 seconds) is a distinguished feature of the passive radar system and especially supports the tracking of such sharp maneuvers.

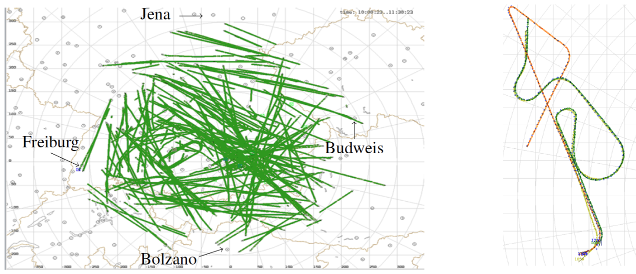

Fig. 5. Air target situation picture and dogfight of three fighter aircraft.

References

[1] M. Cherniakov, Bistatic Radar: Principle and Practice. Wiley, 2007.

[2] N. J. Willis and H. D. Griffiths, Advances in Bistatic Radar. SciTech Publishing, 2007.

[3] M. Edrich, S. Kloeck, and S. Stroth, "A passive radar system for long range air surveillance," SET-241 9th NATO Military Sensing Symposium, Quebec, 2017.

[4] D. Fränken, O. Zeeb, "Real-Time Creation of a Target Situation Picture with the HENSOLDT Passive Radar System.", Proceedings 21st ISIF International Conference on Information Fusion (FUSION), pp. 513-519, 2018.

[5] M. Daun and R. Kaune, "Gaussian mixture initialization in passive tracking applications," 13th Conference on Information Fusion (FUSION), Edinburgh, July 2010.

[6] M. Brötje and W. Koch, "Multistatic tracking for passive radar applications," in Novel radar techniques and applications, vol. II, R. Klemm et al. (eds.), SciTech Publishing, 2017, pp. 335–372.

[7] M. Wiedmann, R. Deininger, R. Schröder, and R. Zimmermann, "Multi transmitter fusion for tracking in a network of transmitters of opportunity," SET-169-41 8th NATO Military Sensing Symposium, Friedrichshafen, 2011.

[8] M. Daun, U. Nickel, and W. Koch, "Tracking in multistatic passive radar systems using DAB/DVB-T illumination," Signal Processing, vol. 92, no. 6, pp. 1365–1386, June 2012.

[9] D. Fränken, S. Stroth, and O. Zeeb, "Tracking and data fusion in a passive radar system," SET-241 9th NATO Military Sensing Symposium, Quebec, 2017.

Barrier Sliding Mode Control for a Hydraulic Actuated Crane

Ismael Castillo[a]

An implementation scheme of independent joint control for a four-degree-of-freedom heavy-duty hydraulic actuated crane is proposed. The implementation consists of two Sliding Mode Controllers with variable barrier function gains (BSMC): Barrier First Order Sliding Mode Control (BFOSMC) and Barrier Super-Twisting Algorithm (BSTA) which allow robust tracking of a with alleviation of high frequency oscillations. Experimental results are presented to show the effectiveness of the proposed semi-automation scheme, exploiting the forestry application motivated low accuracy requirement.

Model. The i-th link system dynamics ([2, 5]) for independent joint control is

$$\begin{aligned} \dot{x}_{1i} &= x_{2i} \\ \dot{x}_{2i} &= m_i(q)^{-1}\left(\lambda_i(x_{pi})x_{3i} + f_{li}\right) \\ \dot{x}_{3i} &= \beta\left[-\lambda_i(q_i)x_{2i}\varphi_{0i} + \varphi_{1i}\nu_i\right], \end{aligned}$$

$$\begin{aligned} \varphi_{0i} &= \tfrac{A_{ai}^2}{V_{ai}(x_{pi})} + \tfrac{A_{bi}^2}{V_{bi}(x_{pi})}, \varphi_{1i} = \tfrac{A_{ai}}{V_{ai}(x_{pi})}\phi_{ai} + \tfrac{A_{ai}}{V_{ai}(x_{pi})}\phi_{bi}. \\ \phi_{ai} &= c_{sai}\sqrt{p_s - p_{ai}}\tfrac{\mathrm{sign}(x_{si}+1)}{2} - c_{ati}\sqrt{p_{ai} - p_t}\tfrac{\mathrm{sign}(x_{si}-1)}{2}, \\ \phi_{bi} &= c_{bti}\sqrt{p_{bi} - p_t}\tfrac{\mathrm{sign}(x_{si}+1)}{2} - c_{sbi}\sqrt{p_s - p_{bi}}\tfrac{\mathrm{sign}(x_{si}-1)}{2}. \end{aligned}$$

x_{1i}, x_{2i} are the i-th generalized coordinates. x_{3i} is the hydraulic force, $\lambda_i(q_i) = \frac{dx_{pi}}{dx_{1i}}$ maps the linear piston force to the generalized force. m_i is a diagonal element of the inertia matrix, f_l are the lumped terms of unmodeled dynamics or external perturbations. A_{ai} and A_{bi}, p_{ai} and p_{bi}, $V_{ai}(x_{pi})$ and $V_{bi}(x_{pi})$ are transversal areas, pressures and volumes of the chambers A and B, respectively. β is the bulk modulus, $c_{sai}, c_{bti}, c_{ati}, c_{sbi}$ constant uncertain coefficients depending on many physical parameters; p_s and p_t are the pressures of supply and tank, respectively. The control input ν_i after compensation of dead zone effect.

Control Design. *Hydraulic Force Dynamics as Singular Perturbations:* Due to the big magnitude in some parameters as bulk modulus $\beta \approx 1.7 \times 10^9$Pa in equation $\dot{x}_{3i}$, the *quasi-steady-state model* ([1]) can be reduced as

$$\dot{x}_{1i} = \frac{\varphi_{0i}}{\lambda_i(q_i)\varphi_{1i}}\psi(u_i). \tag{1}$$

Trajectory Tracking. For a given desired trajectory x_{1di}, tracking error is $e_i = x_{1i} - x_{1di}$, and its dynamics as

$$\dot{e}_i = \frac{\varphi_{0i}}{\lambda_i(q_i)\varphi_{1i}}\nu_i - \dot{x}_{1di}. \tag{2}$$

Barrier Sliding Mode Controllers.

	BFOSMC [4]	BSTA [3]
Barrier Gain	$K_{lb}(e_i) = \alpha_{fi}\ln\left(\frac{\epsilon}{\epsilon - \lvert e_i\rvert}\right)$	$L_b(e_i) = \alpha_{si}\frac{\lvert e_i\rvert}{\epsilon - \lvert e_i\rvert}$
Parameters	$\alpha_{fi} > 0,\ \epsilon > 0$	$\alpha_{si} > 0,\ \epsilon > 0,\ h_1 = 1.5,\ h_2 = 1.1$
BSMC	$\nu_i(e_i) = -K_{lb}(e_i)\mathrm{sign}(e_i),$	$\nu_i(e_i) = -h_1 L_b(e_i)\lvert e_i\rvert^{\frac{1}{2}}\mathrm{sign}(e_i) + \eta_i$ $\dot{\eta}_i = -h_2 L_b^2(e_i)\mathrm{sign}(e_i).$

[a]Institute of Automation and Control, Graz University of Technology, Inffeldgasse 21b/II, 8010 Graz, Austria, E-mail: `i.castillo@tugraz.at`

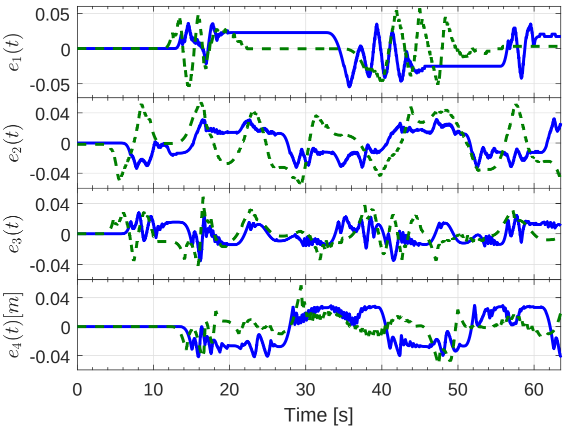

(a) BFOSMC (solid) and BSTA (dashed) tracking errors.

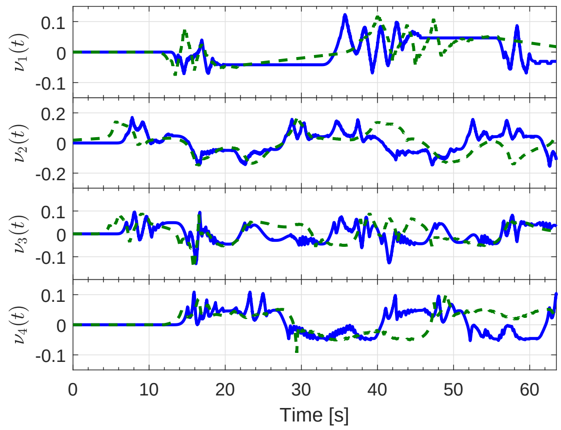

(b) BFOSMC (solid) and BSTA (dashed) control signals ν_i.

Results. The experiments were performed in an electro-hydraulic actuated crane 370RCR manufactured by Cranab AB. The tracking errors are shown in Fig. 1a for BFOSMC, and BSTA, respectively. The continuous control signal ν_i generated by the BSMC are depicted in Fig. 1b for BFOSMC and BSTA, respectively. Note that in both cases, the control signal generated by the BSMC are continuous and the performance was successful for the low accuracy application requirement. It is worth to note that any physical parameter of the crane were taken into account in the controller design.

Conclusions. The robust and not oscillatory (*chattering free*) independent joint control of the 4-DoF hydraulic actuated crane was possible to achieve due to the the gain weakening property at the origin of two Barrier Gain based Sliding Mode Controllers in spite of the high complexity of the mathematical model and the big amount of uncertain parameters. The simplicity of the algorithms is remarkable in comparison with other several proposed methods that rely on the knowledge of the system parameters which makes necessary the usage of identification parameter algorithms.

[1] Hassan K Khalil. Noninear systems. *Prentice-Hall, New Jersey*, 2(5):5–1, 1996.

[2] Herbert E Merritt. *Hydraulic control systems*. John Wiley & Sons, 1967.

[3] Hussein Obeid, Leonid Fridman, Salah Laghrouche, Mohamed Harmouche, and Mohammad Ali Golkani. Adaptation of levant's differentiator based on barrier function. *International Journal of Control*, 91(9):2019–2027, 2018.

[4] Hussein Obeid, Leonid M Fridman, Salah Laghrouche, and Mohamed Harmouche. Barrier function-based adaptive sliding mode control. *Automatica*, 93:540–544, 2018.

[5] Carlos Vazquez, Stanislav Aranovskiy, Leonid Freidovich, and Leonid Fridman. Second order sliding mode control of a mobile hydraulic crane. In *53rd IEEE conference on decision and control*, pages 5530–5535. IEEE, 2014.

Part III.

Wednesday afternoon session

Backstepping Induced Variable Gain Sliding Mode Control

Lars Watermann[a] **Markus Reichhartinger**[b] **Johann Reger**[a]

We consider a second order system of the form

$$\dot{x}_1 = x_2 + \delta_1(t)\varphi(x_1) \tag{1}$$

$$\dot{x}_2 = u + \delta_2(t) \tag{2}$$

with the states $x_1(t), x_2(t) \in \mathbb{R}$ and the control input $u(t) \in \mathbb{R}$. The disturbances $\delta_1(t)$ and $\delta_2(t)$ are assumed to be unknown, but uniformly bounded by

$$|\delta_1(t)| \leq \overline{\delta}_1, \quad \text{and} \quad |\delta_2(t)| \leq \overline{\delta}_2.$$

Let $\varphi : \mathbb{R} \to \mathbb{R}$ be $\mathcal{C}^1$ and known with $\varphi(0) = 0$, such that the unmatched uncertainty $\delta_1(t)\varphi(x_1)$ vanishes at the origin. In this contribution we present a state feedback that asymptotically stabilizes the origin of (1), (2) in the presence of the unknown disturbances.

The backstepping algorithm is a well-known, structured procedure to synthesize nonlinear control laws, see e. g. [4]. The idea is, in a first step, to regard x_2 as an auxiliary control input denoted by $\alpha(x_1)$. The origin $x_1 = 0$ of subsystem (1) is then stabilized with $\alpha(x_1)$ using a control Lyapunov function $V_1(x_1)$. The control law $\alpha(x_1)$ renders $\dot{V}_1 \leq W_1(x_1) < 0 \; \forall \, x_1 \neq 0$. In a second step, V_1 establishes the control Lyapunov function $V = V_1(x_1) + V_2(x_2 - \alpha(x_1))$ which we use to design the control law to render $(x_1, x_2) = (0, 0)$ asymptotically stable. The control input u is then chosen such that $\dot{V} \leq W_1(x_1) + W_2(x_1, x_2) < 0 \; \forall \, (x_1, x_2) \neq (0, 0)$.

The backstepping procedure has already been merged with sliding mode control techniques in various publications. Nevertheless, most of the contributions, e. g., [1] and [2], consider a separated design process, where a backstepping algorithm is terminated after the last-but-one step and a classical sliding mode control law is simply added in the last step in order to obtain certain robustness properties. In [3] and [5] a combined backstepping sliding mode design process is presented where the Lyapunov function is further extended in terms of the sliding variable. The main idea of the presented approach is to use a "full" backstepping algorithm which leads to a discontinuous control law through the choice of W_1 and W_2. The sliding mode control is hence not separated from the backstepping design, but may be considered a consequence.

Main Result. For the control Lyapunov function $V = V_1 + V_2$ we choose

$$V_1 = \frac{k_1}{b}|x_1|^b, \qquad \text{and} \qquad V_2 = \frac{1}{c}|x_2 - \alpha(x_1)|^c, \qquad \text{with} \qquad k_1 > 0, \, b \geq 1, \, c \geq 1 \tag{3}$$

and bound $\dot{V}(x, t) \leq W_1(x) + W_2(x) < 0$ such that

[a]Fachgebiet Regelungstechnik, Technische Universität Ilmenau, Helmholtzplatz 5, D-98693 Ilmenau, E-Mail: {lars.watermann,johann.reger}@tu-ilmenau.de

[b]Institute of Automation and Control, Graz University of Technology, Inffeldgasse 21b/II, 8010 Graz, Austria, E-mail: markus.reichhartinger@tugraz.at

$$W_1(x) = -k_1 k_{11}|x_1|^b - k_1 \left(k_{12} - \overline{\delta}_1\right) |x_1|^{b-1} |\varphi(x_1)|, \tag{4}$$

$$W_2(x) = -|x_2 - \alpha(x_1)|^{c-1} \left(k_2 - \overline{\delta}_2 + \left(k_{12} - \overline{\delta}_1\right) \left|\frac{\partial\alpha(x_1)}{\partial x_1}\varphi(x_1)\right|\right), \tag{5}$$

where $k_{11} > 0$, $k_{12} \geq \overline{\delta}_1$ and $k_2 > \overline{\delta}_2$. Then the origin of system (1), (2) is robustly asymptotically stable with the control law[1]

$$u = -\left(k_2 + k_{12}\left|\frac{\partial\alpha(x_1)}{\partial x_1}\varphi(x_1)\right|\right) \lfloor x_2 - \alpha(x_1)\rceil^0 + \frac{\partial\alpha(x_1)}{\partial x_1} x_2 - k_1 \lfloor x_1\rceil^{b-1} |x_2 - \alpha(x_1)|^{2-c}, \tag{6}$$

$$\alpha(x_1) = -k_{11}x_1 - k_{12} \lfloor x_1\rceil^0 |\varphi(x_1)|, \quad \frac{\partial\alpha(x_1)}{\partial x_1} = -k_{11} - k_{12} \lfloor x_1\rceil^0 \lfloor\varphi(x_1)\rceil^0 \frac{\partial\varphi(x_1)}{\partial x_1}. \tag{7}$$

Note that $\frac{\partial\alpha(x_1)}{\partial x_1}$ in (7) exists due to the properties of φ. The first term of (6) is a variable gain sliding mode control law. The state-dependent gain guarantees robustness against the disturbance $\delta_1(t)\varphi(x_1)$, while the constant gain k_2 handles the matched disturbance $\delta_2(t)$.

The last term of (6) is the compensation of a mixed term that appears through the backstepping design process. To guarantee boundedness of the control input the choice of c is further limited to $1 \leq c \leq 2$ and for simplicity $b = c = 2$ is a reasonable choice. The mixed term can be completely omitted in the special case $b = 1$ and $k_2 > \overline{\delta}_2 + k_1$ without compromising asymptotic stability.

In contrast to most other (backstepping) sliding mode control designs, we present a Lyapunov function that covers the whole closed loop dynamics, i. e., the proof of stability is not divided into reaching phase and sliding phase. The existence of such a Lyapunov function might be of further interest when it comes to adaptive controller design based on the certainty equivalence principle, as already applied in [3] and [5].

[1] G. Bartolini, A. Ferrara, L. Giacomini, and E. Usai. A Combined Backstepping/Second Order Sliding Mode Approach to Control a Class of Nonlinear Systems. In *IEEE International Workshop on Variable Structure Systems*, pages 205–210, 1996.

[2] A. Ferrara and L. Giacomini. Control of a Class of Mechanical Systems With Uncertainties Via a Constructive Adaptive/Second Order VSC Approach. *Journal of Dynamic Systems, Measurement, and Control*, 122(1):33–39, 1998.

[3] Ali Jafari Koshkouei and Alan S.I. Zinober. Adaptive Output Tracking Backstepping Sliding Mode Control of Nonlinear Systems. In *IFAC Robust Control Design*, pages 167–172, 2000.

[4] Miroslav Krstić, Ioannis Kanellakopoulos, and Petar V. Kokotović. *Nonlinear and adaptive control design*. Wiley, 1995.

[5] M. Ríos-Bolívar, A. S. I. Zinober, and H. Sira-Ramírez. Dynamical adaptive sliding mode output tracking control of a class of nonlinear systems. *International Journal of Robust and Nonlinear Control*, 7(4):387–405, 1997.

[1] We use the notation $\lfloor x\rceil^\beta = \mathrm{sign}(x)|x|^\beta$.

Fixed-time parameter estimation under lack of persistency of excitation

Juan G. Rueda-Escobedo[a]

One of the main tasks in adaptive control is parameter identification [7, 11, 5], either for the purpose of control or observation. In many of these cases the identification problem can be expressed in the so called linear regression form $y(t) = C(t)\theta$, where the unknown parameters are contained in the vector $\theta \in \mathbb{R}^n$ and the signals $y(t) \in \mathbb{R}^m$ and $C(t) \in \mathbb{R}^{m\times n}$ are assumed either known or measured. It is well known that the identifiability of the parameters depends, in this case, exclusively on the properties of the *regressor* $C(t)$. Necessary and sufficient conditions for the identifiability of the parameters can be given in terms of the integral of $C(t)$ as in [6] or in a Gramian form as in [1].

The classical way of estimating the unknown parameters is by means of a linear gradient algorithm defined by the differential equation [7]:

$$\dot{\hat{\theta}}(t) = -\Gamma\, C^\top(t)(C(t)\hat{\theta}(t) - y(t)),$$

where $\hat{\theta}(t)$ represents the estimate of θ and $\Gamma \in \mathbb{R}^{n\times n}$ is a positive definite matrix representing the gain of the algorithm. The uniform asymptotic convergence of the algorithm depends in this case of the regressor being *persistently exciting* [6]. However, in practice, it is difficult to guarantee the latter property because it would require that a given system does not attain a stationary operation point. This is why non-uniform convergence of the gradient algorithm has been investigated as early as the 70s [6, Sec. 4]. Very recently, the interest on this problem has resurged motivated by the works [9, 3], and also partially by the introduction of a variation of the linear gradient algorithm in [2, 4]. In all these cases it has been shown that although the regressor may vanish, the "energy supplied" by it should not be finite, that is, the regressor should not belong to $\mathcal{L}_2$ in order to guarantee convergence of the estimation algorithm.

In this contribution we revisit a variation of the fixed-time convergent estimation algorithm introduced in [8], described by the following set of equations:

$$\begin{aligned}
\dot{\hat{\theta}}(t) &= -\Gamma\, N(t)\left(\left\lceil N(t)\hat{\theta}(t) - \psi(t)\right\rfloor^{p_1} + \left\lceil N(t)\hat{\theta}(t) - \psi(t)\right\rfloor^{p_2}\right),\\
\dot{N}(t) &= -N(t)Q\,N(t) + C^\top(t)C(t),\ N(t_0) = 0,\\
\dot{\psi}(t) &= -N(t)Q\,\psi(t) + C^\top(t)y(t),\ \psi(t_0) = 0,
\end{aligned} \tag{1}$$

with exponents $p_1 \in [0, 1)$, $p_2 > 1$ and positive definite matrices $\Gamma \in \mathbb{R}^{n\times n}$, $Q \in \mathbb{R}^{n\times n}$. In [8] (see also [10]) it has been shown that if $C(t)$ is of persistent excitation, then $\hat{\theta}(t)$ converges to θ in fixed-time, uniformly in t_0. In this contribution it is shown that if the regressor is not persistently exciting, but contains "sufficiently enough energy", then the algorithm converges

[a]Control Systems and Network Control Technology, Brandenburg University of Technology Cottbus – Senftenberg, D-03046 Cottbus, Germany. E-mail: ruedaesc@b-tu.de

(non-uniformly) in fixed-time. In contrast with the methods described above, in the present case the regressor may possess finite energy, that is, it is allowed to belong to $\mathcal{L}_2$.

[1] B. O. Anderson. Exponential stability of linear equations arising in adaptive identification. *IEEE Transactions on Automatic Control*, 22(1):83–88, February 1977.

[2] S. Aranovskiy, A. Bobtsov, R. Ortega, and A. Pyrkin. Performance enhancement of parameter estimators via dynamic regressor extension and mixing*. *IEEE Transactions on Automatic Control*, 62(7):3546–3550, July 2017.

[3] Nikita Barabanov and Romeo Ortega. On global asymptotic stability of $\dot{x} = -\phi\,\phi^\top x$ with ϕ not persistently exciting. *Systems & Control Letters*, 109:24 – 29, 2017.

[4] A. Belov, S. Aranovskiy, R. Ortega, N. Barabanov, and A. Bobtsov. Enhanced Parameter Convergence for Linear Systems Identification: The DREM Approach*. In *2018 European Control Conference (ECC)*, pages 2794–2799, June 2018.

[5] Petros A. Ioannou and Jing Sun. *Robust adaptive control*. Prentice Hall, Upper Saddle River, NJ, 1996.

[6] A. Morgan and K. Narendra. On the uniform asymptotic stability of certain linear nonautonomous differential equations. *SIAM Journal on Control and Optimization*, 15(1):5–24, 1977.

[7] K. S. Narendra and A. M. Annaswamy. *Stable Adaptive Systems*. Prentice Hall, Englewood Cliffs, New Jersey 07632, 1989.

[8] M. Noack, J. G. Rueda-Escobedo, J. Reger, and J. A. Moreno. Fixed-time parameter estimation in polynomial systems through modulating functions. In *2016 IEEE 55th Conference on Decision and Control (CDC)*, pages 2067–2072, Dec 2016.

[9] Laurent Praly. Convergence of the gradient algorithm for linear regression models in the continuous and discrete time cases. Research report, PSL Research University ; Mines ParisTech, Feb 2017.

[10] Juan G. Rueda-Escobedo. *Finite-time observers for linear time-varying systems and its applications*. PhD thesis, Universidad Nacional Autónoma de México (UNAM), Ciudad Universitaria, CDMX, México, Aug 2018. Available at: http://132.248.9.195/ptd2018/agosto/0778889/Index.html.

[11] Shankar Sastry and Marc Bodson. *Adaptive Control: Stability, Convergence, and Robustness*. Prentice-Hall, Englewood Cliffs, New Jersey 0763, 1989.

Optimal Feedback Controllers‘ Design Based on Evolutionary Computation with Differential Evolution

Andrej Sarjaš[a] **Dušan Gleich**[a]

1 Introduction

The feedback controller design procedure requires sufficient knowledge about the controlled plant dynamics. The real plant dynamics are mostly presented with a set of linear or nonlinear differential or difference equations, which represent the real system with a certain amount of uncertainty. Models used in control design are an approximation of systems, and are subject to different external disturbances and parameters‘ uncertainty. The model uncertainties and disturbances are the challenge of many linear, as well as nonlinear, controller paradigms, where the optimization procedure has an essential role in defining the relevant parameters of the selected controller and feedback structure. Evolutionary Computation approaches offer many algorithms and procedures which can tackle many optimization problems in various fields, such as Engineering, Statistics, and Science. The given talk discusses the optimization procedure with Differential Evolution for a different kind of feedback controller designs.

2 Differential Evolution

Differential Evolution (DE) was introduced by R. Storn and K. Price [2].

Since then, DE has attracted many researchers, and has been applied in numerous applications. Today, DE is one of the most efficient optimizers, with relatively simple structure, and can solve a wide range of optimization problems[1]. DE performs well in both global and local searches, and can find an optimum solution without getting trapped in local minima. From the engineering point of view it is straightforward to use, and may be applied to the large-scale, as well as to the multi-objective optimization problems.

The basic principle of DE is the introduction of a new computational scheme to generate trial parameter vectors. The new trial parameter vectors are the sum of a randomly selected population member and the weighted difference of two randomly selected members. This stage of the algorithm is also known as a Differential Mutation (DM), and is the core and specialty of the DE. After the mutation, the crossover procedure follows. The crossover operator promotes the population diversity, where the new resultant vector contains the elements of parents and DM vectors. The final stage of DE is selection and further progression. The selection consists of comparing an offspring with its parent, which induces local elitism and

[a]Institut of Automation, University of Maribor, Koroška cesta 46, 2000 Maribor, Slovenia, E-mail: andrej.sarjas@um.si, dusan.gleich@um.si

still maintains the population spread. If the newly generated vector has a lower value of the Objective Function than the randomly selected parents‘ vector, they will replace the parents in a new population, otherwise it will be discarded. The DE procedure continues until the predefined objective is met.

3 Feedback controller design and DE optimization procedure

The feedback controller synthesis can be a challenging task, especially if the feedback system needs to fulfill various physical and design constraints. The quality of the feedback system can be denoted as the ability of the controller to ensure proper dynamic performance, sufficient disturbance rejection, and uncertainty suppression. Heuristic optimization for feedback controller design can be used from various aspects and for different control paradigms, such as the pole assignment approach,$H_\infty \backslash H_2$ robust control, nonlinear control approaches, trajectory planning, stability assessment, etc. [3],[4].The given presentation will cover some approaches and practical examples of the controller design with DE parameter optimization in the next fields:

- Optimal H_∞ controller design with a fixed controller structure
- Backstepping controller design with an optimal selection of the controller parameters with regard to the closed loop performance characteristics
- Selection of Sliding mode controller parameters with a preselected performance index

References:

[1] S. Das and P. N. Suganthan. Differential evolution: A survey of the state-of-the-art. *IEEE Transactions on Evolutionary Computation*, 15(1):4–31, Feb 2011.

[2] K. V. Price. Differential evolution: a fast and simple numerical optimizer. In *Proceedings of North American Fuzzy Information Processing*, pages 524–527, June 1996.

[3] Uroš Sadek, Andrej Sarjaš, Amor Chowdhury, and Rajko Svečko. Fpga-based optimal robust minimal-order controller structure of a dc–dc converter with pareto front solution. *Control Engineering Practice*, 55:149 – 161, 2016.

[4] Andrej Sarjaš, Amor Chowdhury, and Rajko Svečko. Multi-criteria optimal pole assignment robust controller design for uncertainty systems using an evolutionary algorithm. *International Journal of Systems Science*, 47(12):2792–2807, 2016.

Synchronization of the gas production and utilization rates of a solid-to-gas process and a downstream gas-to-X process

Thomas NIGITZ[1,2] tel: +43 316 873 9247, fax: +43 316 873 9247, email: thomas.nigitz@bioenergy2020.eu
Markus GÖLLES[1,2] tel: +43 316 873 9208, fax: +43 316 873 9202, email: markus.goelles@bioenergy2020.eu
Christian AICHERNIG[3] tel: +43 1 2161895 502, fax: -, email: c.aichernig@repotec.at
Hermann HOFBAUER[1,4] tel: +43 1 58801 30010, fax: +43 1 58801 915001, email: hermann.hofbauer@tuwien.ac.at
Martin HORN[1,2] tel: +43 316 873 7025, fax: +43 316 873 7028, email: martin.horn@tugraz.at

1 BIOENERGY 2020+ GmbH, Graz, Austria
2 Institute for Automation and Control, Graz University of Technology, Graz, Austria
3 Aichernig Engineering GmbH, Vienna, Austria
4 Institute for Chemical, Environmental and Bioscience Engineering, Vienna University of Technology, Vienna, Austria

Introduction, process description and aim of this work

A promising approach in process engineering is the conversion of solids into gas that can then be easier transported and further processed to valuable products. An example is the valorisation of biomass or waste. As the solids’s properties like size, shape and composition typically vary, the conversion rate strongly varies. However, the downstream gas-to-X process typically requires well-defined inlet parameters to create their product X. Thus, the amounts of gas produced by the solid-to-gas process and demanded by the downstream gas-to-X process have to be synchronized.

The synchronization of the solid-to-gas process and the gas-to-X process is typically realized as visualized in Figure 1. The solid-to-gas process produces a surplus of gas, so that at any time the demand of the gas-to-X process is met. The remaining gas, i.e. the respective surplus, is burned in a gas-to-heat process.

This is ensured by a PI-controller controlling the pressure between the processes by actuating the position of a valve in order to adjust the amount of gas burned in the gas-to-heat process. The average amount of gas fed to the gas-to-heat process is typically controlled by actuating the screw feeding the solids to the solid-to-gas process. However, this often goes along with stability issues, since two separate controllers act via two different actuators (fuel feed and valve at the inlet of the gas-to-heat process) on the same controlled variable, the pressure between the reactors. For this reason, in many applications the fuel feed is very often only manually controlled by the plant operators, leading to a substantial increase of operational expenses.

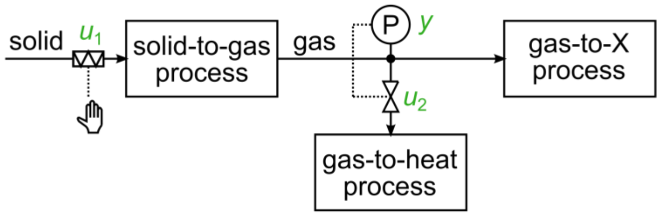

Figure 1: Process structure

Furthermore, burning the gas in the gas-to-heat process only provides heat, what is a low quality product compared to the products resulting from typical gas-to-X processes. For that reason, the amount of gas burned in the gas-to-heat process should be as small as possible. In summary, the current control strategy for this synchronization requires manual adjustments at the solid-to-gas process and large amounts of gas are burned in the gas-to-heat process.

For this reason, the aim of the work presented is to develop a novel control strategy for the synchronization of the production and utilization rates of a solid-to-gas process and a downstream gas-to-X process. The novel control strategy should achieve at least the control quality of the control strategy currently applied, but without the necessity of manual adjustments of the fuel feed by the operators and with less gas burned in the gas-to-heat process. However, the configuration under consideration is generally only used on an industrial scale; otherwise the processes cannot be operated economically. Thus, the control strategy should be limited to PID-controllers and their extension by static functions. Furthermore, the control strategy should be able to get implemented during normal plant operation, but the operation of the plant must not be disturbed, i.e. no experiments can be performed and the controllers need to be tuned appropriately in advance.

Model for controller design

The plant is modelled via a linear MISO-system with two manipulating variables, the speed of the screw and the position of the valve. The screw acts on the controlled variable, the pressure between the reactors, through the solid-to-gas process, which is modelled via a first-order system P_1. The valve acts significantly faster on the controlled variable, but its action is inverted. Thus, its action on the controlled variable is modelled via a negative static gain P_2. In most practical implementations the pressure signals are already digitally filtered to hide the high-frequency fluctuations which cannot be avoided anyway, and very often it is required by the operators that these filters must not be removed. Thus, a digital filter F is applied before the controlled variable is available for the controller. This digital filter is modelled as a first-order low-pass filter. So, the controlled system consists of a first-order system and a static gain in parallel, both with a first-order system in series.

The model parameters are derived from a complex simulation model of the industrial plant. As no experiments are possible, the complex simulation model bases on physical and chemical considerations, and only measurement data from normal plant operation is used to set the operating point of the plant in the complex simulation model.

Controller design

The novel control strategy controls the pressure y by actuating both manipulating variables u_i. The amount of gas burned can be lowered on average, if it only has to compensate high frequency fluctuations. This motivates the separation of the control task in frequency domain. The low frequency components of the control error are controlled via the screw u_1. And its high frequency components are controlled via the valve u_2. The two manipulating variables are actuated by individual PID-controllers C_i as visualized in Figure 2. In detail, an I-controller C_1 acts u_1 and a PD-controller C_2 acts on u_2. In practical application the operating point of u_2 is set by a constant offset added to the PD-controllers output.

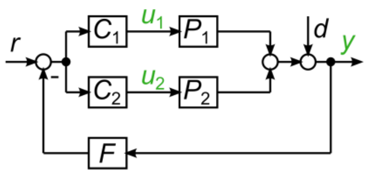

Figure 2: Control structure

The control strategy needs to suppress disturbances d around the operating point of the plant. Thus, the two controllers are parameterized using the sensitivity function $S: d \to y$. Since the current control strategy suppresses disturbances sufficiently well, the two controllers are parameterized so that their total sensitivity function is close to the sensitivity function of the current control strategy.

Experimental validation

The novel control strategy was validated at a representative industrial plant. For this purpose, it was implemented at a standard PLC allowing bumpless switching from and to the current control strategy. Then the plant was operated with the novel control strategy for several hours. Within this test different sets of control parameters were applied and evaluated. During this validation the solid-to-gas process was operated automatically and the amount of gas burned in the gas-to-heat process was lowered significantly.

Conclusions

The synchronization of the gas production and utilization rates of a solid-to-gas process and a gas-to-X process can be improved by the novel control strategy, which consists of simple PID-controllers and proved its applicability in an experimental validation at a representative industrial plant. This increases the competitiveness of industrial plants using this process structure.

Institute of Automation and Control
Graz University of Technology

21st Styrian Workshop on Automatic Control

September 9-11, 2019, Schloss Retzhof, Austria

CONFERENCE PROGRAM

Monday Sep 9, 2019

17:00 – 18:00	Registration
18:00	Dinner

Tuesday Sep 10, 2019

08:30 – 08:40	Opening
08:40 – 09:20	Jakob Rehrl, Selma Celikovic, Martin Kirchengast, Stephan Sacher, Julia Kruisz, Johannes Khinast, Martin Horn *Implementation of Model-based Control Concepts in Continuous Pharmaceutical Engineering*
09:20 – 10:00	Daniel Ritzberger, Stefan Jakubek *Data-driven modelling of Polymer Electrolyte Membrane Fuel cells for Fault Detection*
10:00 – 10:30	Coffee Break
10:30 – 11:10	Klemens Kranawetter, Richard Seeber, Robert Bauer, Martin Horn *Adaptive Resonance-Suppression for Automotive Test Bed Systems*
11:10 – 11:50	Thomas Nigitz, Markus Gölles, Christian Aichernig, Hermann Hofbauer, Martin Horn Synchronization of the gas production and utilization rates of a solid-to-gas process and a downstream gas-to-X process
11:50 – 12:30	Stefan Richter *Systematic and Efficient Decision Making with Optimization*
12:45 – 14:30	Lunch
14:45 – 22:00	Social Program (bus leaves at 2:45 pm)

Wednesday Sep 11, 2019

08:30 – 09:10	Milad Gholami, Alessandro Pilloni, Alessandro Pisano, Elio Usai *Robust consensus-based Secondary Frequency and Voltage Restoration of Inverter-based Islanded Microgrids*
09:10 – 09:50	Daipeng Zhang, Johann Reger *Parameter Preference for the Super-Twisting Algorithm Induced by H_{inf}-Norm Analysis*
09:50 – 10:30	Nicole Gehring, Richard Kern *An infinite-dimensional Output Feedback Tracking Controller for a Pneumatic System with Distributed Parameters*
10:30 – 11:00	Coffee Break
11:00 – 11:40	Dietrich Fränken, Oliver Zeeb *Passive Radar for Air Surveillance*
11:40 – 12:20	Alberto Ismael Castillo Lopez *Barrier Sliding Mode Control for a Hydraulic Actuated Crane*
12:30 – 14:00	Lunch
14:00 – 14:40	Lars Watermann, Markus Reichhartinger, Johann Reger *Backstepping Induced Variable Gain Sliding Mode Control*
14:40 – 15:20	Juan G. Rueda-Escobedo *Fixed-time Parameter Estimation Under Lack of Persistency of Excitation*
15:50 – 16:30	Andrej Sarjaš, Dušan Gleich *Optimal Feedback Controllers' Design Based on Evolutionary Computation with Differential Evolution*